frontiers in Marine Science

ORIGINAL RESEARCH
published: 07 June 2019
doi: 10.3389/fmars.2019.00264

Microzooplankton Distribution and Dynamics in the Eastern Fram Strait and the Arctic Ocean in May and August 2014

Peter J. Lavrentyev[1,2]*, *Gayantonia Franzè*[1†] *and Francisco B. Moore*[1]

[1] *Department of Biology, The University of Akron, Akron, OH, United States,* [2] *Department of Zoology, Herzen Russian State Pedagogical University, Saint Petersburg, Russia*

Microzooplankton community structure, distribution, growth, and herbivory were examined in the eastern Fram Strait and Arctic Ocean shelf affected by the Atlantic water inflow in May (during the spring bloom) and August (post-bloom, summer stratification) 2014. In May, integrated microzooplankton biomass in the upper 100 m ranged from 0.16 g C m^{-2} above the slope to 2.3 g C m^{-2} within the West Spitsbergen Current (0.71 g C m^{-2} on average), where it peaked in the mixed layer at 206 μg C L^{-1}. This is the highest volumetric microzooplankton biomass recorded so far in the Arctic. It primarily consisted of mixotrophic oligotrich ciliates from the genus *Strombidium,* which were dominant in the spring and formed a surface bloom (79 × 10^3 cells L^{-1}). The heterotrophic dinoflagellates *Gyrodinium* and *Protoperidinium* were abundant at the diatom-dominated stations in the ice-covered waters during both seasons. In the summer, a more diverse community included a large proportion of heterotrophic and mixotrophic dinoflagellates, tintinnids, and other ciliates. Microzooplankton biomass increased to the average of 1.27 g C m^{-2}. At the ice-covered and open water stations in the Yermak shelf and deep basin, microzooplankton grew at 0.04 to 0.38 d^{-1}; their species-specific growth rates were up to 1.79 d^{-1}. Microzooplankton herbivory on average removed 72% (in two experiments > 100%) of daily primary production with the exception of samples dominated by *Phaeocystis pouchetii* colonies. The results indicate that microzooplankton play a significant role in the carbon cycle in this Atlantic-influenced polar system.

Keywords: microzooplankton, herbivory, growth, mixotrophy, Arctic Ocean

OPEN ACCESS

Edited by:
Jacob Carstensen,
Aarhus University, Denmark

Reviewed by:
Kalle Olli,
University of Tartu, Estonia
Lumi Haraguchi,
Aarhus University, Denmark

***Correspondence:**
Peter J. Lavrentyev
peter3@uakron.edu

***Present address:**
Gayantonia Franzè,
Institute of Marine Research,
Flødevigen, Norway

Specialty section:
This article was submitted to Global Change and the Future Ocean, a section of the journal Frontiers in Marine Science

Received: *11 December 2018*
Accepted: *02 May 2019*
Published: *07 June 2019*

Citation:
Lavrentyev PJ, Franzè G and Moore FB (2019) Microzooplankton Distribution and Dynamics in the Eastern Fram Strait and the Arctic Ocean in May and August 2014. Front. Mar. Sci. 6:264. doi: 10.3389/fmars.2019.00264

INTRODUCTION

Rapid warming is occurring in the Arctic (IPCC, 2013), where average temperatures have risen twice as fast as those elsewhere in the world (Corell, 2006). The warming trend has resulted in widespread reductions in Arctic ice cover (Kwok and Rothrock, 2009). Sea ice is the central component of the polar environment and its alternations translate global warming to marine ecosystems, including changes in biological productivity, food web structure, and the biogeochemical cycles (Wassmann and Reigstad, 2011; Wassmann and Lenton, 2012). An extended

open-water period in the Arctic Ocean is projected to boost pelagic primary production (Slagstad et al., 2011; Brown and Arrigo, 2012) and increase the role of small-sized phytoplankton (Li et al., 2009). The non-linear nature of ecosystem response to climate change complicates predictions. Understanding and predicting its effects at the system level requires insight into the coupled nature of physical and biological interactions.

An area of special interest in the marine ecosystem studies is carbon flow through pelagic food webs. Even minor climate effects at the lower trophic levels get amplified in food chains (Sarmento et al., 2010) with significant effects at the higher trophic levels, which are critically dependent on the efficient energy transfer (McBride et al., 2014). In the world ocean, microzooplankton (*sensu lato* phagotrophic protists between 15 and 300 μm, including heterotrophic and mixotrophic ciliates, dinoflagellates, and sarcodines) are main consumers of phytoplankton production (Calbet and Landry, 2004; Schmoker et al., 2013). Recent data show that microzooplankton are a key component of pelagic food webs in productive Arctic shelf systems, such as the Bering Sea (Sherr et al., 2013; Stoecker et al., 2014a) and the Barents Sea (Franzè and Lavrentyev, 2014, 2017).

The Atlantic water is the primary source of heat in the Arctic (Polyakov et al., 2012). Its inflow has intensified (Schauer et al., 2004) and temperature has increased over the last several decades (Lind and Ingvaldsen, 2012). The Fram Strait, a 2500-m deep and 500-km wide passage between the Greenland shelf and Spitsbergen, connects the Atlantic and Arctic Oceans (Cokelet et al., 2008). The eastern Fram Strait is dominated by the West Spitsbergen Current (WSC) – a northward continuation of the Norwegian Atlantic Current and the main conduit of Atlantic Water in the Arctic Ocean (Pnyushkov et al., 2015). In addition, WSC is transporting large quantities of Atlantic phyto- (Paulsen et al., 2016) and zooplankton into the Arctic Ocean (Kosobokova and Hirche, 2009; Basedow et al., 2018).

The Fram Strait is already one of the most productive areas of the Arctic (Slagstad et al., 2011) and is likely become a regional hotspot with increased primary production due to efficient transport of nutrients and the increased light availability in the ice-free water column (Randelhoff et al., 2018). However, microzooplankton remain little studied in this polar region. In the northwestern Fram Strait, dominated by the cold East Greenland Current, heterotrophic and mixotrophic ciliates and dinoflagellates were abundant in the early spring (Seuthe et al., 2011). In the central Fram Strait and the waters north of Spitsbergen, despite considerable ciliate biomass, microzooplankton herbivory was found to be insignificant during the late stages of phytoplankton bloom dominated by the prymnesiophyte *P. pouchetii* (Calbet et al., 2011).

The central goal of our study was to determine microzooplankton quantitative importance in the pelagic food webs within the WSC and the Arctic Ocean shelf affected by the Atlantic water inflow. Extreme seasonality in light typical for the Arctic and strong variability in the sea ice melt across the Fram Strait create a very dynamic and spatially heterogeneous environment. Therefore, we focused our study on two critical phases of the annual cycle: the spring bloom and summer stratification. The study specific questions were: (1) what is the spatial distribution of microzooplankton biomass and major taxonomic groups? (2) What is the capacity of microzooplankton to use primary production? (3) What are the growth and production rates of microzooplankton?

The Study Sites

The study was conducted in the eastern Fram Strait during the Carbon Bridge cruises aboard the R/V *Helmer Hansen* in May and August 2014 (**Figure 1**). Samples were collected along two longitudinal transects named C (79.4°N) and D (79.0°N). These transects extended between 10 and 4°E and crossed the warm core of WSC. During both cruises the dominating water mass in the upper 500 m of these transects was Atlantic (Basedow et al., 2018). Its inflow rate did not differ substantially between May and August compared to winter. In May 2014, the Atlantic water (3.5–5.0°C) reached up to the surface between 6 and 8°E. In the western end of transect D, colder, lower-salinity surface waters were observed west of 5°E, closer to the sea ice edge. In August 2014, a fresher (salinity < 34) surface layer extended over most of transect D, with surface temperatures ranging from 7.5°C in the east to 1°C west of 4°E (Randelhoff et al., 2018).

At the shelf break, three ice-covered sites designated further as the process (i.e., experimental) stations were sampled in the inflow region west (P3, P4) and northwest (P1/P5) of Spitsbergen in May (**Table 1**). In August, we sampled two process stations in the ice fields north of Spitsbergen: P6, representing the deep Arctic basin, and P7, which was selected to represent the area of AW inflow close to the shelf slope. One of the spring process stations (P1/P5), now ice-free, was also sampled in August. See Randelhoff et al. (2018) for a detailed treatment of hydrographic conditions at the process stations.

MATERIALS AND METHODS

Sea temperature and salinity were measured with a Seabird 911 Plus CTD system. Raw fluorescence was measured with the attached fluorometer. Samples were collected from different depths: 2, 5, 10, 20, 30, 40, 50, 100 m and the deep chlorophyll layer (DCL) using Niskin bottles mounted on a rosette. The transect samples were not replicated because it would require three separate CTD casts at each station and wire time was limited during the cruises. Subsamples for examining microzooplankton and chlorophyll concentrations were immediately collected and preserved as described below.

All glass- and plastic ware, and tubing were cleaned with 10% HCl, deionized water, and 0.2-μm filtered seawater prior to sampling. Experimental containers were handled using gloves. For experimental samples, freshly collected seawater was carefully siphoned into a 20 L polycarbonate carboy using submerged silicone tubing, which had one end wrapped in a 153 μm mesh. The collected samples were taken to a shipboard temperature-controlled cold room. All experimental manipulations were conducted at ± 1°C ambient sea temperature under dim light. The growth and grazing mortality rates of phytoplankton rates were measured using two-point dilution (Landry et al., 2008). Instead of linear

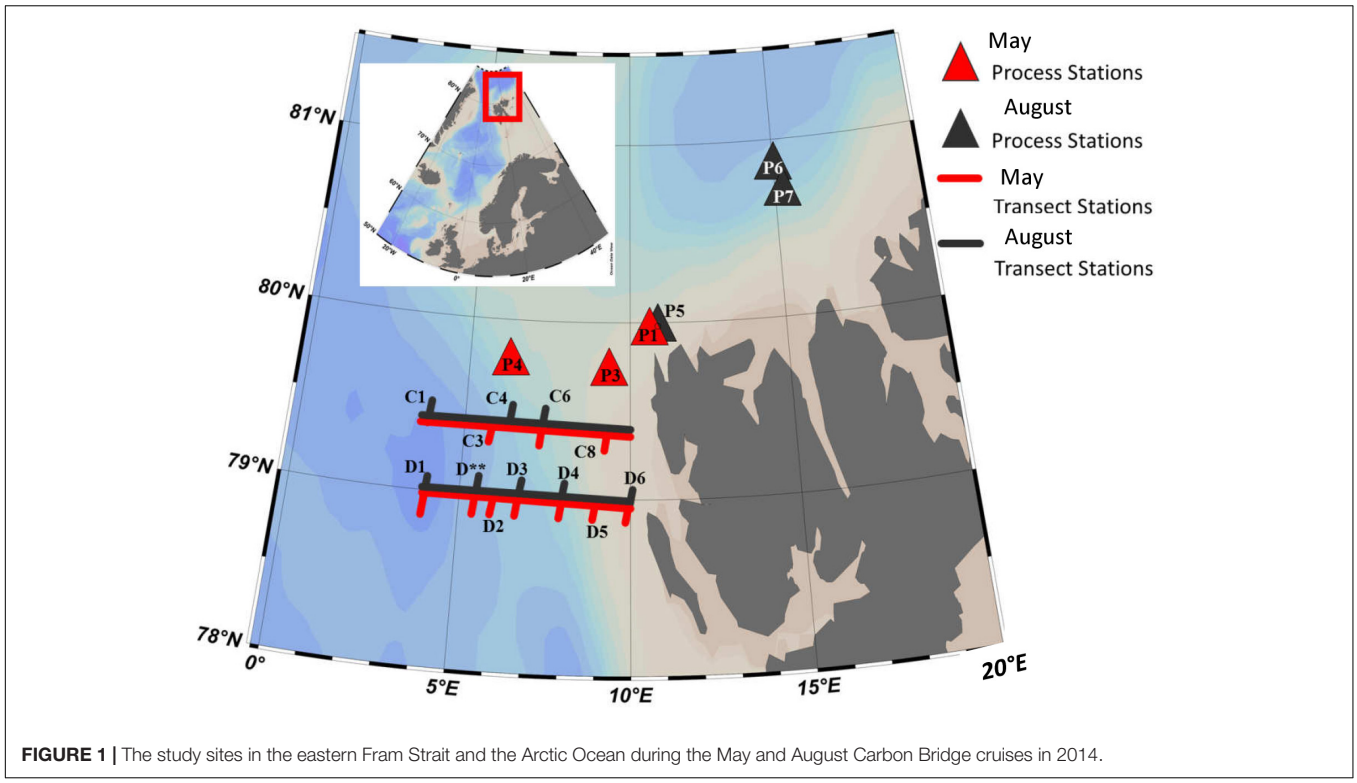

FIGURE 1 | The study sites in the eastern Fram Strait and the Arctic Ocean during the May and August Carbon Bridge cruises in 2014.

TABLE 1 | Abiotic conditions at the process stations and phytoplankton growth and grazing mortality rates in May and August 2014.

Station	Date	Ice cover	Sample depth (m)	T (°C)	Salinity	Chl ($\mu g\ l^{-1}$)	Growth (μ, d^{-1})	*SD= standard deviation*	Grazing mortality (g, d^{-1})	*SD*	*g*/μ
P1/P5	5/19/2014	25%	1	0.0	34.5	5.19	0.27	0.08	0.12	0.03	0.44
P1/P5	5/19/2014		10	−0.5	34.8	5.54	0.31	0.03	0.17	0.01	0.55
P3	5/23/2014	85%	15	0.0	34.2	4.88	−0.24*	0.06	–	–	–
P3	5/23/2014		40	3.0	35.1	4.32	−0.15	0.04	0.17	0.10	–
P4	5/25/2014	40%	1	−1.0	33.7	3.58	0.14	0.05	0.22	0.04	1.57
P4	5/25/2014		15	0.2	34.2	5.20	−0.07	0.03	0.21	0.01	–
P1/P5	8/9/2014	0%	1	6.0	34.9	0.76	0.24	0.06	0.16	0.07	0.67
P1/P5	8/9/2014		18	6.3	34.9	1.05	0.22	0.05	0.08	0.02	0.36
P6	8/12/2014	90%	1	−1.0	31.9	0.13	0.22*	0.08	–	–	–
P6	8/12/2014		25	5.5	34.2	0.95	0.42	0.09	0.29	0.08	0.69
P7	8/14/2014	70%	1	−0.5	31.7	0.16	0.33	0.07	0.40	0.11	1.21
P7	8/14/2014		14	5.0	34.8	0.34	0.37	0.10	0.24	0.01	0.65

**Calculated from the whole seawater treatment.*

regression, this method estimates the grazing mortality rate (g) as the difference in phytoplankton growth (μ) between the whole seawater and highly diluted treatments. The diluted treatment approximates "no grazing." We used this method due to its efficiency and the ability to provide the rates, which are not statistically different from those estimated by the multi-point method (Strom and Fredrickson, 2008; Chen, 2015) even when non-linear responses are taken into account (Morison and Menden-Deuer, 2017).

Seawater was added to 0.6 L Nalgene clear glass bottles. The diluted treatments were prepared by mixing nine parts filtered seawater (0.2 μm large volume Pall Science pleated capsules using gravity flow) with one part whole seawater to yield a 10% dilution. The capsules were pre-soaked in 5% HCl and thoroughly rinsed with deionized water prior to use. To equalize plankton growth conditions, all triplicated diluted and undiluted samples were amended with dissolved nutrients to final concentrations of 16 μM N (KNO_3 + NH_4Cl; 15:1 based on N) and 1 μM P (K_2HPO_4). These additions correspond to the maximum concentrations of nutrients found in the Fram Strait deep waters (1000 m) during the Carbon Bridge project (15.7 μM NO_3 and 1.07 μM PO_3, Randelhoff et al., 2018).

An additional triplicated set of the whole seawater controls was left unfertilized to test the effect of nutrient additions on phytoplankton growth. All bottles were screened with neutral density filters to mimic light conditions at a certain depth (70 to 4% surface irradiance). Surface samples were incubated on the deck in an open plastic container with running surface seawater for 24 h. The bottles were periodically rotated by hand to avoid particle settling. Samples from deeper layers were incubated in a temperature-controlled deck incubator exposed to natural light and equipped with a plankton wheel (set at 0.25 revolutions per minute). During the experiments, temperature was monitored and remained within ± 0.5°C of the initial sea temperature. Samples for chlorophyll and microzooplankton counts were collected at T_0 and T_{24}.

Chlorophyll was collected onto 0.2 μm Nylon membrane filters from 250 to 500 ml samples using low vacuum. The filters were frozen and stored in liquid N_2. Extraction was done in 90% acetone for 24 h at −20°C. Turner Designs Trilogy fluorimeter was used to measure chlorophyll concentrations via the acidic method (Arar and Collins, 1997). Microzooplankton were preserved with 2% (final concentration) acid Lugol's iodine, stored at 4°C for 24 h, and post-fixed with 1% (final concentration) formaldehyde. Additional plankton samples were fixed with formaldehyde only (1% final concentration) for examination of chloroplast-bearing microzooplankton.

Microzooplankton were settled from 50 to 100 ml sub-samples and examined under an inverted differential interference contrast microscope equipped with fluorescence at 200x. The entire surface area of Utermöhl chambers was scanned. In some cases, additional sub-samples were examined from each bottle in the experiments. Not fewer than 40 cells were measured with an eyepiece micrometer at 400–600x for each abundant taxon. The cell linear dimensions were converted to volume using approximated geometric shapes. The volumes were then converted to carbon (Putt and Stoecker, 1989; Menden-Deuer and Lessard, 2000). Any ciliates in our samples were counted as microzooplankton, whereas dinoflagellates were included only if their maximum linear dimension was at least >15 μm (Møller et al., 2006). Formaldehyde-only preserved samples were settled and examined similarly using a combination of interference contrast and fluorescence. Ciliates and dinoflagellates with chloroplasts in their cytoplasm were categorized as mixotrophs, and those without chloroplasts as heterotrophs. To calculate the cell chlorophyll quota, we used the chlorophyll vs. volume regression for marine phytoplankton (Montagnes et al., 1994) and assumed that autrophic and mixotrophic plankton have similar cellular chlorophyll content (Dolan and Perez, 2000).

Phytoplankton apparent growth rates were calculated assuming exponential growth: $\mu = \ln(N_t/N_0)/(t/24)$, where: μ = growth rate (d), N_0 and N_t = chlorophyll concentrations at the beginning and end of the experiment, respectively, and t = time (hours). Grazing mortality rates (g) were determined as the difference between μ measured in the diluted ($\mu_{10\%}$) and whole (μ_{WSW}) seawater samples: $g = \mu_{10\%} - \mu_{WSW}$. In the experiments where phytoplankton grew slower in diluted samples, or not significantly different from the whole seawater treatment, g was not calculated (since there can be no negative grazing rate), whereas the growth of phytoplankton was reported from the whole seawater treatment. If chlorophyll concentrations declined in all treatments, phytoplankton decline rate was reported. The average rates used for calculating the grazing to growth ratio (g/μ) calculation did not include the negative values (Stoecker et al., 2014a).

Microzooplankton species-specific instantaneous growth rates (r, d^{-1}) were determined from their initial and final (24 h) concentrations in the triplicated whole seawater control bottles from the simultaneous dilution experiments, assuming exponential growth (Franzè and Lavrentyev, 2014). Microzooplankton community secondary production rates (MzP, $\mu g\ C\ l^{-1}\ d^{-1}$) were determined using the following formula: $MzP = \Sigma\ r \times b_0$, where b_0 is the initial population biomass of individual taxa (Franzè and Lavrentyev, 2017). The community daily growth rate of microzooplankton was as MzP/B_0, where B_0 is total initial community biomass.

To estimate dispersion, we used standard deviation throughout the manuscript unless noted otherwise. All pairwise comparisons of the average values of different plankton parameters (chlorophyll *a*, microzooplankton biomass, and phytoplankton growth and grazing mortality rates) between treatments, stations, and seasons were conducted using a two-tailed *t*-test assuming unequal variances. The effects of seasonality, depth, sea temperature, salinity, and chlorophyll concentrations on the distribution of total microzooplankton biomass and that of different taxonomic-functional groups along Transect D were examined using a general linear model (GLM) multiple regression. The two study seasons, the spring and summer, and the sampling depth were used as factors (i.e., categorical variables) in GLM, whereas the water column characteristics were used as covariates (i.e., continuous independent variables). The sampling depths were designated as the upper (0–30 m) and lower (31–100 m) layers. These categories were chosen based on the vertical distribution patterns of microzooplankton biomass. In addition to these factors we also included their interaction (i.e., season by layer) to improve the overall model fit. Three outlier samples (the highest microzooplankton biomass values in the upper layer at D5 in May) were excluded from the model. Relationships between plankton growth, production, and mortality rates and sea temperature as well as between microzooplankton biomass and production rates were examined using least square linear regression. All statistical analyses were conducted using Minitab 18.

RESULTS

Microzooplankton Biomass Distribution

Microzooplankton biomass in the upper 100 m of Transit D was distributed unequally along the transect (**Figures 2B**, **3B**). It was elevated in the mixed layer at D1 and D3, and reached its maximum for the whole study period at D5 (2306 mg C m^{-2}) mostly due to the mixotrophic oligotrich ciliates *Strombidium* sp. (71000 cells L^{-1}) and *S. conicum* (8000 cells L^{-1}), which formed nearly 90% of total ciliate biomass (206 $\mu g\ C\ L^{-1}$) near

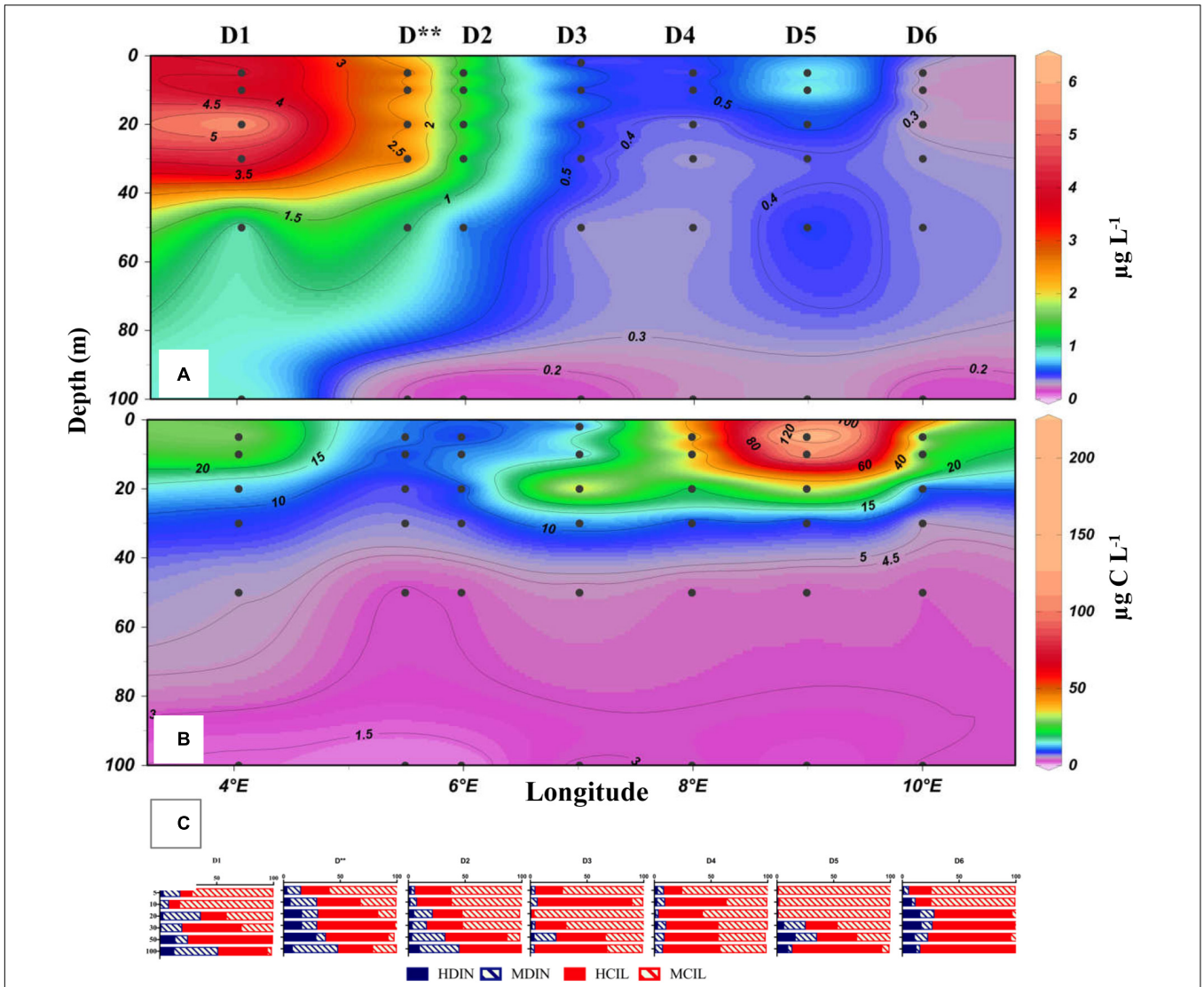

FIGURE 2 | The distribution of chlorophyll *a* **(A)**, microzooplankton biomass **(B)**, and the relative biomass **(C)** of mixotrophic ciliates (MCIL) and dinoflagellates (MDIN) and heterotrophic ciliates (HCIL) and dinoflagellates (HDIN) in the upper 100 m of the water column along the D transect during the May 2014 Carbon Bridge cruise.

the surface (**Figure 2C**). Overall, the average depth-integrated microzooplankton biomass in the upper 100 m in transect D in May was 713 mg C m^{-2}. Similar microzooplankton composition was recorded at the process sites P and Transect C (**Figures 4**, **5**), but microzooplankton biomass in the latter transect was much lower than in Transect D (<10 µg C L^{-1} at C3 and C8). Microzooplankton also accumulated at certain depths, which were not included in the vertical sampling routine. For example, at P1 in May, microzooplankton biomass reached 43 µg C L^{-1} at 15 m, mostly due to mixotrophic ciliates, and only 10.1 and 1.3 µg C L^{-1} at 10 and 20 m, respectively. Because the 15 m sample was collected separately for incubation, it was not included in the integrated biomass.

Excluding its peak values at D5 in May, microzooplankton biomass was generally higher in August at all studied locations with an increased proportion of dinoflagellates. In Transect D, microzooplankton peaked at D3 in the mixed layer (**Figure 3B**) but overall was distributed evenly along the transect compared to May. Its depth-integrated biomass in the upper 100 m averaged 1270 mg C m^{-2}. The most pronounced seasonal changes were observed at C sites (**Figure 5**), where total microzooplankton biomass increased 3–4 times and dinoflagellates 5–10 times in August compared to May. At the process stations the seasonal trend was similar: depth-integrated microzooplankton biomass (0 to 100 m) increased from 250 to 400 to >1200 mg C m^{-2}.

Microzooplankton Composition

In addition to the mixotrophic oligotrichs, heterotrophic dinoflagellates, such as *Gyrodinium spirale, Protoperidinium bipes,* and *Gymnodinium* sp. were also a significant component of microzooplankton population at the ice-edge and ice-covered

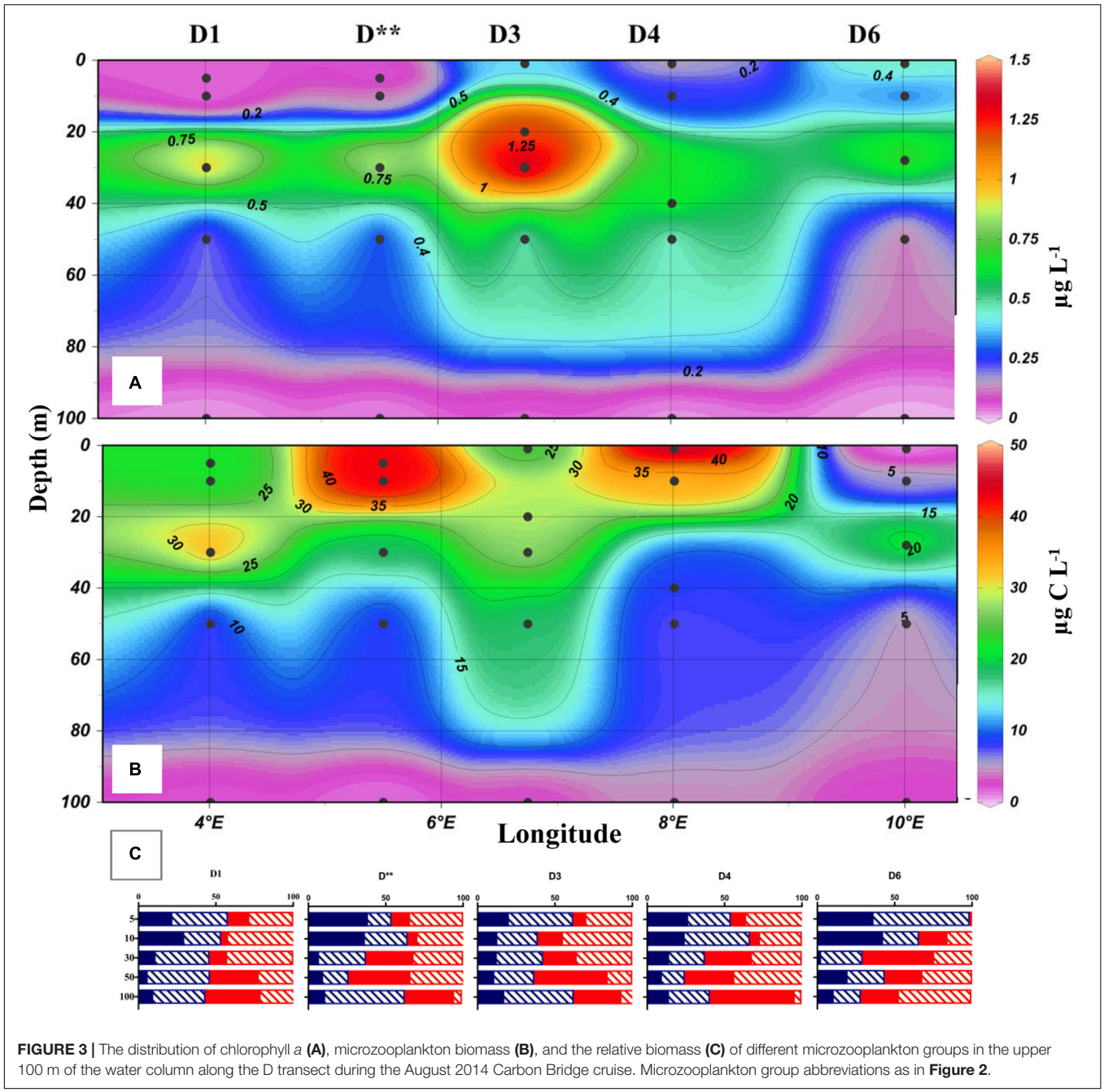

FIGURE 3 | The distribution of chlorophyll *a* **(A)**, microzooplankton biomass **(B)**, and the relative biomass **(C)** of different microzooplankton groups in the upper 100 m of the water column along the D transect during the August 2014 Carbon Bridge cruise. Microzooplankton group abbreviations as in **Figure 2**.

waters. The kleptoplastidic (e.g., Peltomaa and Johnson, 2017) cyclotrichid ciliate *Mesodinium rubrum* was omnipresent, but only at relatively low abundance (<500 cells L^{-1}, except P3 surface 1120 cells L^{-1}). The heterotrophic choreotrich ciliates *Lohmaniella oviformis* and *Pelagostrobilidium neptuni* were distributed more evenly in the water column and their relative biomass increased at medium depths along with several mixotrophic gymnodiniids.

In August, microzooplankton composition was more diverse (**Figure 3C**). In addition to the species present in the spring assemblage, we also found a diversity of mixotrophic and heterotrophic dinoflagellates such as *Ceratium arcticum* (*Tripos arcticus*), *Gymnodinium* spp., *Protoperidinium* sp., *Gyrodinium fusiforme*, *Amphidinium* spp., *Dinophysis rotundata*, *Torodinium robustum*, *Pronoctiluca pelagica*. Ciliate biomass was dominated by the mixotrophic oligotrich *Tontonia appendiculariformis* and also included several other mixotrophic (*Laboea strobila, Strombidium lynni, Didnidium gargantua, M. rubrum*) and heterotrophic species (*S. acuminatum*, *Leegardiella sol*, *Balanion comatum*, *Balanion planktonicum*, *M. acarus*, *Urotricha* sp., *U. globose, Astylozoon faurei*). In addition, several tintinnid ciliates were also present including *Parafavella faureii* (the most

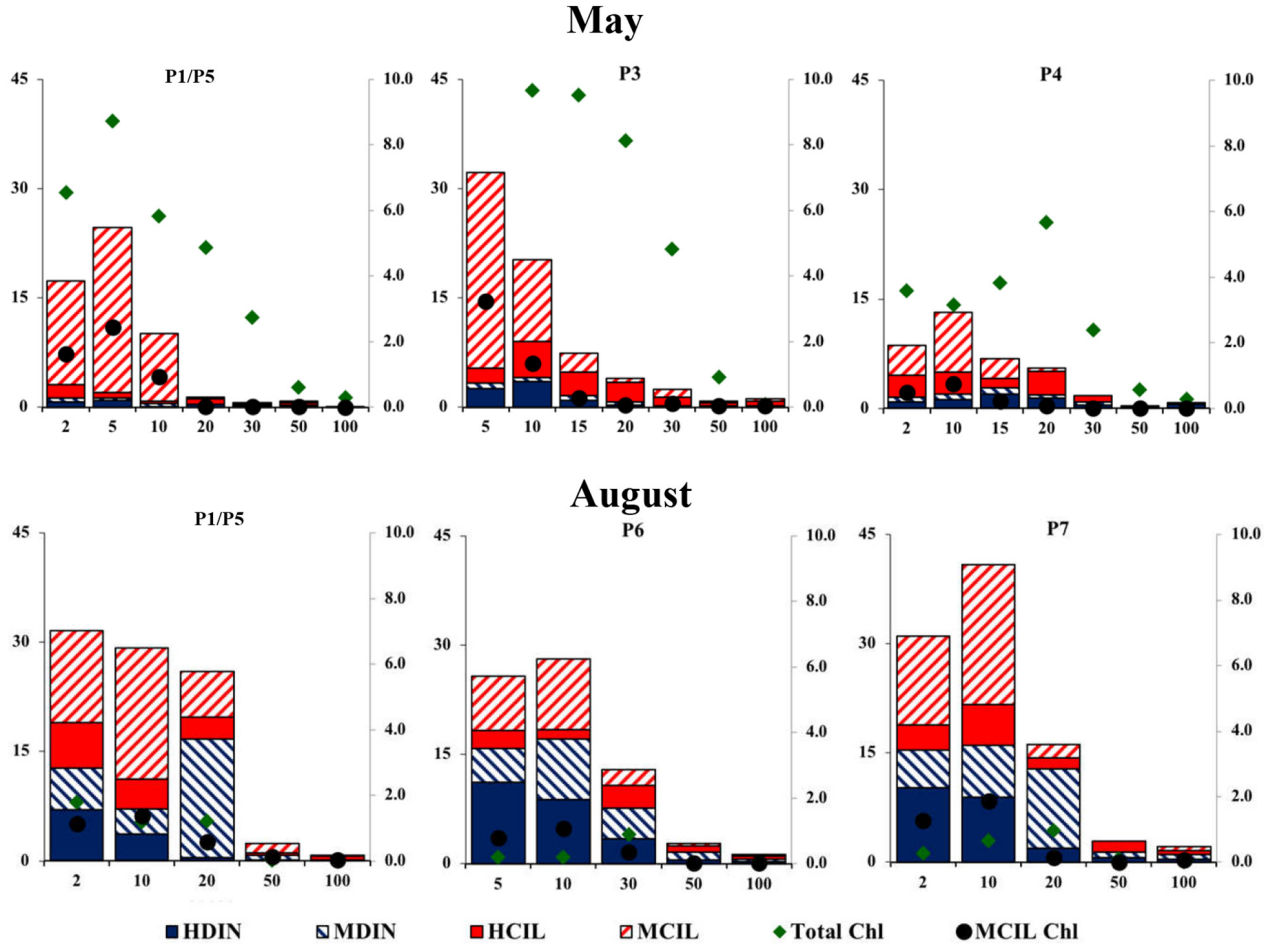

FIGURE 4 | The distribution of chlorophyll, mixotrophic ciliate chlorophyll, and biomass of different microzooplankton at the process stations in May and August 2014. Microzooplankton group abbreviations are as in **Figure 2**. Total Chl = the concentration of extracted chlorophyll; MCIL Chlx10 = calculated mixotrophic ciliate chlorophyll multiplied by 10.

common in our samples), *Acanthostomella norvegica*, *Ptychocylis obtusa*, *Salpignella* sp., and *Leprotintinnus pellucidus*.

Total and Mixotrophic Chlorophyll *a* Distribution

During the May cruise, the highest chlorophyll values (**Figure 2A**) were found in the western end of Transect D (Stations D1, D**), where diatoms and *P. pouchetti* formed a bloom at the ice edge. At D3, D4, and D6 chlorophyll remained < 1 μg L^{-1}. At the process stations further north, chlorophyll was high (up to 13.5 μg L^{-1}) and concentrated in the shallow mixed layer (**Figure 4**). A bloom of *P. pouchetii* accompanied by diatoms was also in progress, especially at P3. The colonial prymnesiophyte contributed 80–90% of phytoplankton abundance in the ice-covered waters (based on light microscopy, Sanz-Martín et al., 2018). In the summer a DCL at around 20–30 m was present along transect D. Nevertheless, chlorophyll concentrations were much lower in August (**Figure 3A**) than in May. Similar patterns were observed in Transect C and at the process stations with the exception of P1/P5 (**Figures 4**, **5**). Under the ice, diatoms were the dominant group in August (70–80% phytoplankton abundance, Sanz-Martín et al., 2018) with a lesser contribution from *P. pouchetii*.

The average ratio of calculated mixotrophic chlorophyll to total extracted chlorophyll in the surface layer along Transect D was 19% in May and 43% in August (**Figure 6**). The same ratio for depth-integrated values in the upper 50 m was 10 and 9% in May and August, respectively. These average values do not include station D5 in May, where calculated integrated mixotrophic chlorophyll was 83% of total concentration and the ratio in the surface layer exceeded 100% due to the bloom of two mixotrophic oligotrichs. The calculated contribution of *Strombidium* sp. (cell volume 15.5×10^3 μm^3, chlorophyll content 30 pg $cell^{-1}$) alone was ∼2 μg L^{-1}. At C sites, the ratio increased from $< 2\%$ in May to 20–50% in the surface layer and 6–18% in the DCL in August (**Figure 5**, absolute values are shown). At the process stations there was an opposite trend despite a decrease in total chlorophyll (**Figure 4**). The ratio declined from 7 to 8% in

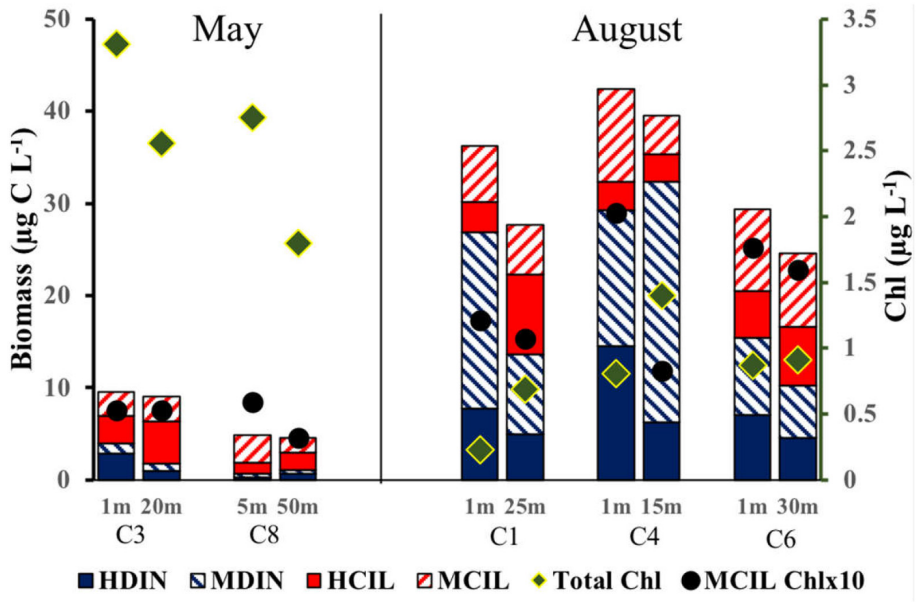

FIGURE 5 | The distribution of chlorophyll (Total Chl), mixotrophic ciliate chlorophyll (MCIL Chl) and biomass of different microzooplankton groups along at selected transect C stations in May and August 2014. Microzooplankton group abbreviations are as in **Figure 2**. Chlorophyll abbreviations as in **Figure 4**.

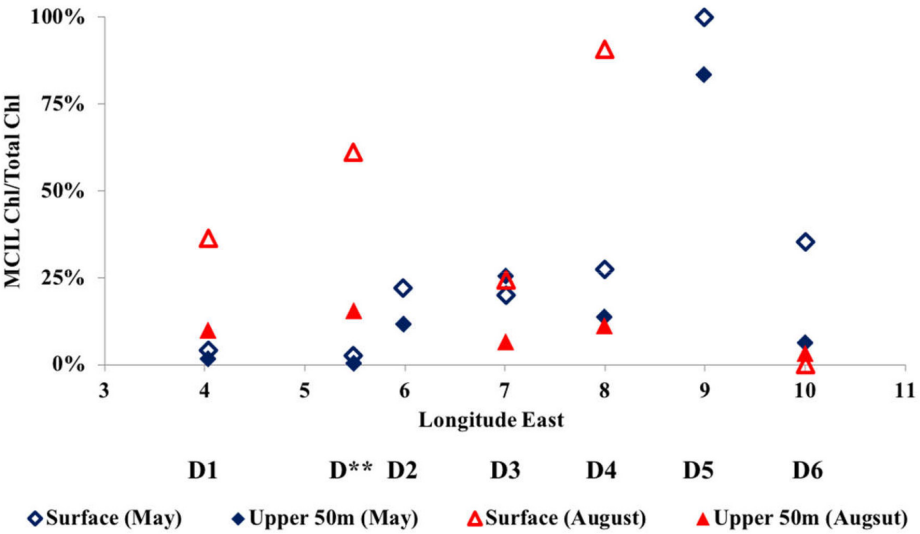

FIGURE 6 | The distribution of the mixotrophic ciliate chlorophyll to total chlorophyll ratio in the surface and the upper 50 m along the D transect in May and August 2014.

the mixed layer in May to 2–3% in August due to the lower abundance of mixotrophic oligotrichs.

The Effects of Environmental Factors on Microzooplankton Distribution

Sampling depth was the only factor that significantly influenced the distribution of total microzooplankton biomass. It also had pronounced effects on different microzooplankton components (mixotrophic and heterotrophic ciliates and mixotrophic and heterotrophic dinoflagellates): they all decreased with depth (**Table 2**). With the exception of mixotrophic ciliates, all microzooplankton groups were also influenced by seasonality: their biomass increased in the summer. Sea temperature was negatively related to microzooplankton biomass, but its effect was significant only for total microzooplankton and mixotrophic dinoflagellates. Heterotrophic ciliate biomass was positively related to salinity and chlorophyll, but only the former relationship was significant. Overall, the multiple regression model

TABLE 2 | General linear model of microzooplankton biomass distribution vs. season, depth, and environmental parameters along Transect D (n = 63).

		Responses				
		MZP	**HDIN**	**MDIN**	**HCIL**	**MCIL**
	Model r^2:	48.5	60.0	76.6	35.0	18.2
	Constant	−79.0	59.7	−30.0	−63.8	−45.0
	p-Value	0.57	0.062	0.237	0.005	0.70
Factors						
Season	*F*-value	10.6	5.7	45.4	12.2	1.33
	p-Value	***0.002***	0.02	***<0.001***	***0.001***	0.25
	Coef. spring	***−9.05***	−1.50	***−3.38***	***−1.54***	−2.65
	Coef. summer	9.05	1.50	3.38	1.54	0.254
Layer	*F*-value	18.3	6.16	34.9	11.4	6.60
	p-Value	***<0.001***	***0.016***	***<0.001***	***0.001***	***0.013***
	Coef. upper	***9.21***	***1.23***	***2.29***	***1.15***	***4.57***
	Coef. lower	***−9.21***	***−1.23***	***−2.29***	***−1.15***	***−4.57***
Season * Layer	*F*-value	***7.31***	***6.25***	***37.6***	***7.86***	0.52
	p-Value	***0.01***	***0.015***	***<0.001***	***0.007***	0.47
	Coef. spring upper	−5.13	−1.07	−2.2	−0.84	−1.13
	Coef. spring lower	5.31	1.07	2.2	0.84	1.13
	Coef. summer upper	5.31	1.07	2.2	0.84	1.13
	Coef. summer lower	−5.31	−1.07	−2.2	−0.84	−1.13
Covariates						
Temperature	*F*-value	4.37	2.12	13	2.05	1.39
	p-Value	***0.034***	0.15	***0.001***	0.16	0.24
	Coef.	***−4.67***	−0.72	***−1.39***	−0.48	−2.09
Salinity	*F*-value	0.55	2.86	2.08	8.78	0.23
	p-Value	0.46	0.10	0.155	***0.004***	0.64
	Coef.	3.08	−1.58	1.08	***1.95***	1.64
Chlorophyll *a*	*F*-value	0.33	2.21	0.01	1.94	0.29
	p-Value	0.57	0.143	0.928	0.17	0.59
	Coef.	−0.70	−0.48	−0.02	0.27	−0.54

Coef., coefficient. Layers: Upper 0–30 m, Lower: 31–100 m. Bold and italic indicate significant coefficients in the regression and the corresponding p and F-values.

explained much larger proportion of dinoflagellate biomass variation (77 and 60% of mixotrophs and heterotrophs, respectively) than that of heterotrophic ciliates (35%). Mixotrophic ciliates displayed little connection to the analyzed environmental variables (only 18% of their biomass variation was explained by the model).

Phytoplankton Growth and Grazing Mortality Rates

The results of dilution experiments at the process stations and the corresponding abiotic conditions in May and August are shown in **Table 1**. The chlorophyll values shown in the table are the initial concentrations in the experimental bottles, which were measured after seawater was screened through a 153 μm mesh to remove large zooplankton. The resulting concentrations were typically 92–98% of ambient, but the screening removed almost 40% of chlorophyll at P3-15 m, where colonial *Phaeocystis* was abundant at the time of experiment. At this station, we used an additional carbon filter to remove potential cytotoxins from 0.2-μm filtered seawater (Stoecker et al., 2015). However, following this treatment chlorophyll strongly decreased in the diluted treatment (-0.66 d^{-1}) compared to the whole seawater control (-0.24 d^{-1}). Therefore, the growth rate was calculated from the changes in the latter treatment. The same calculation approach was used at P6-1 m, where the initial concentration of chlorophyll in the whole seawater was too low (0.13 μg L^{-1}) for reliable growth rate estimates in the diluted treatment.

Phytoplankton growth rates were not stimulated by nutrient additions in any of the 12 experiments except in the open surface water sample at P1/P5 in August (data not shown). The rates varied from -0.24 d^{-1} (P3-15 m) to 0.31 d^{-1} (P1-10 m) in May and 0.22 to 0.42 d^{-1} in August. The highest growth rates were recorded in August at sub-zero temperatures, low salinity (<32), and under the dense (70–90%) ice cover. The rates did not correlate with sea temperature (linear regression, r^2 = 0.04, p = 0.56), but tended to increase with the ice cover, although the relationship was not significant (**Figure 7**). We found no difference (t-test, p = 0.4) between the rates in the surface samples and those collected from DCL despite the fact that light conditions during incubations were very different (70 vs. 4% of surface irradiance). The average growth rates (excluding negative values) were 0.24 d^{-1}

in May and 0.30 d^{-1} in August. The corresponding grazing mortality rates measured in 9 out of 12 experiments did not correlate with temperature or chlorophyll either. Herbivory was measurable in two experiments dominated by *P. pouchetii* (P3-40 m and P4-15 m) and significantly increased with the ice cover (**Figure 7**). Overall, the grazing rates were similar in May (0.18 ± 0.05 d^{-1}) and August (0.23 ± 0.12 d^{-1}). In the experiments where both grazing and growth rates were measured, their ratio (g:μ) varied from 0.36 to 1.57. Based on the average growth (0.29 d^{-1}) and grazing (0.21 d^{-1}) rates, microzooplankton herbivory impact at the process stations was 72% of the daily primary production. At sea temperatures above and below 2°C this ratio was 60 and 85%, respectively, although the difference was not statistically significant (*t*-test, $p = 0.25$).

Microzooplankton Growth and Production Rates

The individual species-specific growth rates of microzooplankton taxa were related to temperature. For example, *P. faureii* grew 0.69 d^{-1} at −0.5°C and 1.25 d^{-1} at 3.0°C; *T. appendiculariformis* 0.56 d^{-1} at −1.0°C and 0.69 to 1.25 d^{-1} at 6°C. The fastest growing microzooplankton were the ciliates *M. rubrum* (1.39 d^{-1} at 3°C and 0.92 d^{-1} at 6.3°C) and *B. planktonicum* (1.73 d^{-1} at 6.0°C). Many mixotrophic oligotrichs grew fast at low temperatures: for example, *Strombidium* sp. and *S. conicum* 1.00 d^{-1} at 0 and 0.2°C, resepctively. The growth rate of *G. spirale* initially increased with temperature from 0.42 d^{-1} at −1°C to 1.12 d^{-1} at 0°C, and then declined to 0.84 d^{-1} at 6.3°C.

The average total microzooplankton growth rates (calculated as the daily P/B ratio) were similar between May and August at the process stations: 0.15 ± 0.10 and 0.14 ± 0.12, respectively. At temperatures > 2°C, typical for the Atlantic water, the average daily microzooplankton P/B was 0.23 ± 0.10 d^{-1}.

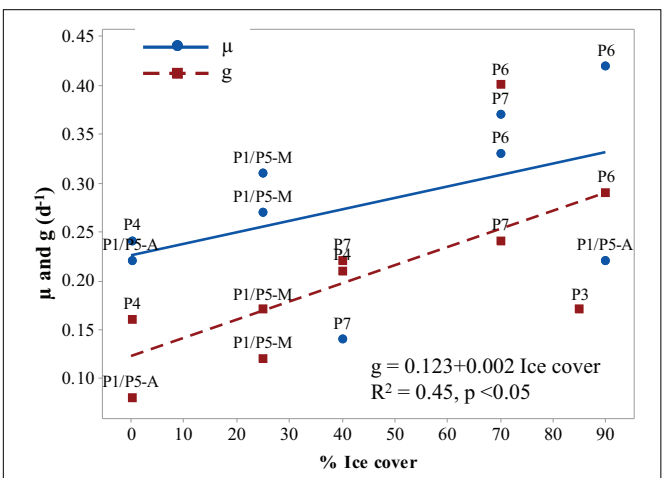

FIGURE 7 | The rates of phytoplankton growth (solid line, circles) and grazing mortality (dashed line, squares) vs. the percentage of sea ice cover at the process stations. P1/P5-M = in May and P1/P5-A = in August.

For those taxa that increased during the experiments, the average taxon-specific growth rates were also similar between the cruises: 0.50 ± 0.19 and 0.40 ± 0.13. The proportion of these taxa in total microzooplankton biomass also did not change between May and August (33 and 31%, respectively), but varied among the experiments (11% at P6-1 m to 75% at P3-40 m). The maximum average species-specific growth (0.78 d^{-1}) was recorded in the latter experiment at 3°C. Both the growing population (**Figure 8A**) and total microzooplankton rates (**Figure 8B**) were positively related to sea temperature with the exception of DCL samples > 5°C in August. Microzooplankton production rate varied from 0.29 μg C L^{-1} d^{-1} at P3-40 m (3°C) to 9.2 μg C L^{-1} d^{-1} at P5-1 m (6.0°C). Production did not correlate with temperature (**Figure 8C**) or chlorophyll ($r^2 = 0.02$, $p = 0.69$), but the initial biomass of growing populations explained a large proportion of productivity variation ($r^2 = 0.84$, $p < 0.001$). The average rates at the process sites were

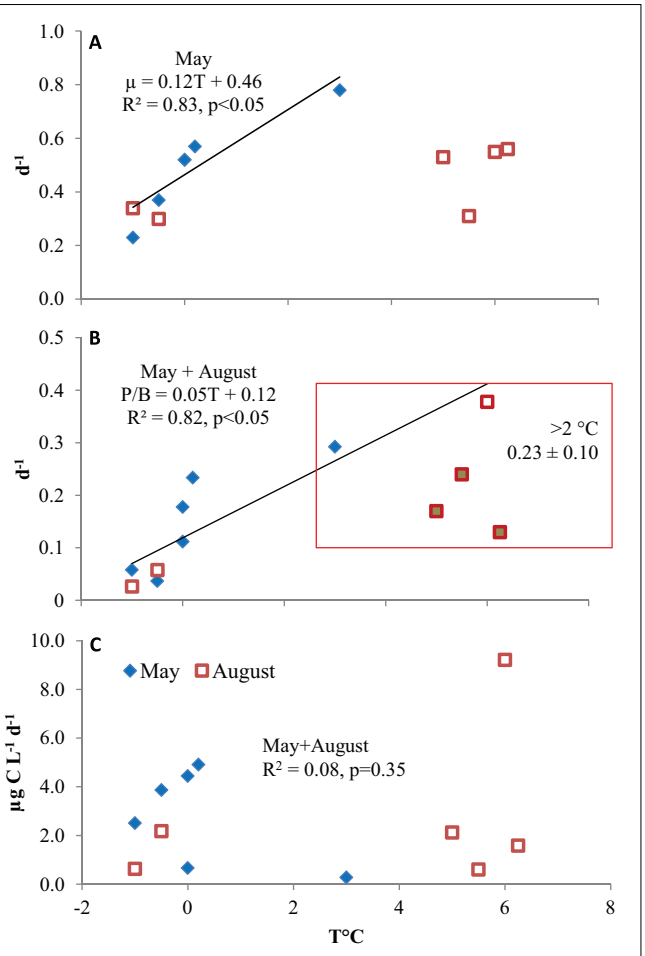

FIGURE 8 | The average growth rates of microzooplankton populations that increased over time in experimental incubations **(A)** and total microzooplankton growth **(B)** vs. sea temperature in May (filled triangles) and August (open squares). Filled squares denote regression outliers. **(C)** Microzooplankton community production.

2.7 ± 1.6 μg C L^{-1} d^{-1} in May and 2.8 ± 3.0 μg C L^{-1} d^{-1} in August.

DISCUSSION

Microzooplankton Distribution and the Controlling Factors

Microzooplankton biomass recorded in this study in the upper 0–50 m layer (175 to 2306 mg C m^{-2}) was considerably higher than previously reported values from the northwestern Fram Strait (47 to 108 mg C m^{-2} in 0–60 m, Seuthe et al., 2011). The average volumetric biomass of 22.6 μg C L^{-1} in this study was similar to the values reported by Calbet et al. (2011) from the central Fram Strait and the Yermak slope in July (20.7 μg C L^{-1}, range 1.84 to 67 μg C L^{-1}). Both studies have indicated considerable heterogeneity in microzooplankton spatial distribution. Similar microzooplankton biomass values were also reported from the productive Arctic shelf seas (Hansen et al., 1996; Rat'kova and Wassmann, 2002; Verity et al., 2002; Lavrentyev, 2012; Stoecker et al., 2014b; Franzè and Lavrentyev, 2017). To our knowledge, the biomass of ciliates in the surface layer at D5 in May (206 μg C L^{-1}) is the highest microzooplankton biomass reported so far from the Arctic. It exceeds the previous record set in the southeast Bering Sea (164 μg C L^{-1} including ciliates and dinoflagellates > 10 μm, Olson and Strom, 2002).

Microzooplankton biomass did not correlate with sea temperature in the northeastern Fram Strait (Seuthe et al., 2011). A negative relationship between total microzooplankton and sea temperature observed in this study was likely due to the fact that microzooplankton increased in August, when their biomass peaked in the cooler surface layer. The positive relationship between heterotrophic ciliates and salinity is probably indirect as well and reflects generally better conditions for this microzooplankton component in the Atlantic waters of WSC. The design of our study was not conducive to isolating the effects of ice cover on microzooplankton distribution and dynamics. Most of our transect stations remained ice-free in the spring and summer, whereas the process stations located further north in the Arctic Ocean were ice-covered during both seasons (except P1/P5 in August). Nevertheless, it should be noted that microzooplankton biomass increased in August in the ice-covered Arctic Ocean waters just like it did in the open Atlantic waters of the eastern Fram Strait. Further, microzooplankton herbivory rates were positively related to the ice cover; the mechanism behind this effect remains to be determined.

Ciliates and dinoflagellates inhabiting polar seas are well-adapted to their cold and icy environment (Sherr et al., 2013; Franzè and Lavrentyev, 2014; Menden-Deuer et al., 2018) and food availability is central among factors controlling their populations dynamics and composition (Caron and Hutchins, 2013). In addition to the distinct vertical patterns, microzooplankton biomass and composition displayed pronounced seasonality. At all examined sites the spring assemblage was dominated by mixotrophic oligotrichs and large heterotrophic dinoflagellates. The latter group is usually associated with diatom blooms in polar waters (Lovejoy et al., 2002; Olson and Strom, 2002; Sherr et al., 2009, 2013; Franzè and Lavrentyev, 2017). As indicated by the results of regression analyses in this study, total chlorophyll may be too crude a measure to describe the specific resource requirements of microzooplankton. An increase in the abundance of *Synechococcus* in the surface layer in August (Paulsen et al., 2016) and the predominance of nanophytolankton typical for the eastern Fram Strait in summer (Nöthig et al., 2015) could have supported higher and more diverse microzooplankton biomass.

Another factor controlling microzooplankton populations in the ocean is crustacean zooplankton predation (Saiz et al., 2013). The dominant Atlantic expatriate *Calanus finmarchicus* and its Arctic congeners *C. hyperboreus* and *C. glacilais* are opportunistic omnivores that feed on both phytoplankton and microzooplankton (Ohman and Runge, 1994; Levinsen et al., 2000a; Campbell et al., 2009). The surface peak of the plastidic oligotrichs in May corresponded to low concentration of mesozooplankton based on the laser optical plankton counter high frequency vertical profiles (Basedow et al., 2018). In addition, the eastern end of transect D is the zone of fast northward AW flow over the shelf (Basedow et al., 2018) and the ciliates could have been advected there. Given their fast specific growth rates in our experiments (>1 d^{-1}), it is also plausible that mixotrophic oligotrichs could have formed a bloom using a temporary relief of top–down control. Inversely, low microzooplankton biomass at C3 and C8 in May could have been due to large *Calanus* spp., which were abundant in the upper part of the water column along transect C. The ratio of microzooplankton biomass (0–100 m) to the biomass of *C. finmarchicus* (0–1000 m) along transect D was 30 to 106% in May and increased to 63 to 123% in August. This ratio demonstrates the quantitative importance of microzooplankton in the eastern Fram Strait. For comparison, the inflow of *C. finmarchicus* with the Atlantic water was estimated to be in the order of 5×10^5 metric tons C y^{-1} (Basedow et al., 2018). At the ice covered process stations, microzooplankton biomass was ca. 40% of *C. finmarchicus* biomass in May and 106% in August (Svensen et al., 2019).

Mixotrophic Microzooplankton and Their Importance

All prior microzooplankton studies in the Fram Strait and the Yermak shelf (Putt, 1990; Calbet et al., 2011; Seuthe et al., 2011) reported significant contribution of mixotrophic ciliates to microzooplankton biomass. Their contribution to total chlorophyll calculated in this study is substantial, particularly in the surface layer. In the adjacent Barents Sea, mixotrophic chlorophyll in DCL varied between 1.5 and 49% (Franzè and Lavrentyev, 2017). In the Bering Sea, ciliate chlorophyll was sometimes over 50% of total chlorophyll (Stoecker et al., 2014a) and 46% in the Kara Sea (Lavrentyev, 2012). In the surface layer at D5 in May, the mixotrophic to total chlorophyll ratio was ∼200%. Obviously, this is an artifact, but not necessarily stemming from our calculations. Vacuum

filtration through membrane filters commonly used to collect chlorophyll may disrupt fragile ciliate cells and thus lead to losses of mixotrophic chlorophyll (Putt, 1990). The estimates of mixotrophic ciliate chlorophyll made in this study should be treated as tentative. Mixotrophic chlorophyll content was calculated based on algal chlorophyll content (Montagnes et al., 1994), assuming that the volume to chlorophyll relationship is similar to that in autotrophic plankton (Dolan and Perez, 2000). The former study was based on cultures growing under controlled conditions and supplied with sufficient nutrients, thus the physiological state (and consequently chlorophyll quotas) of the cells might be different than those observed in the environment. It should be mentioned, however, that the cell chlorophyll quota of *S. conicum* (30,000 μm^3) measured directly in the Barents Sea by Putt (1990) was similar to that estimated in this study using the above assumptions (48 and 55 pg chlorophyll $cell^{-1}$, respectively). The cell chlorophyll content and kleptoplastid numbers vary widely among different marine oligotrichs (Stoecker et al., 1988; McManus et al., 2012) and can depend on the food availability (Schoener and McManus, 2012). The factors controlling physiology, distribution, and dynamics of mixotrophic ciliates remain poorly understood. Although the distribution of mixotrophic ciliates did not correlate with any of the available environmental variables in this study, their peak abundance was found at low chlorophyll concentrations. Similarly, mixotrophic oligotrichs peaked within the Polar Front, which is characterized by low primary productivity in the Barents Sea (Franzè and Lavrentyev, 2017). These observations may suggest that mixotrophy is a response to oligotrophic conditions. On the other hand, dense populations of mixotrophic ciliates were found in the productive regions of the Kara Sea (Lavrentyev, 2012) and the Bering Sea (Stoecker et al., 2014b). Further studies must clarify the role of mixotrophy, which is widespread among planktonic protists in the polar seas (Stoecker and Lavrentyev, 2018). In general, this trophic mode enhances carbon flow through pelagic food webs by compensating for respiratory losses (Ward and Follows, 2016).

Microzooplankton Herbivory

Planktonic copepods have been considered the main herbivores in the marine food webs (Smetacek, 1999). In contrast to this traditional concept, recent research indicates that copepods primarily rely on ciliates and other microzooplankton as an essential food source except during diatom blooms (Saiz and Calbet, 2011; Ray et al., 2016). Due to their relatively slow growth and long life histories (Hop et al., 2006; Litchman et al., 2013), copepods cannot provide a rapid response to unicellular phytoplankton growth in the spring. On an annual basis the combined grazing by *Calanus* spp. and euphausids amounts to ca. 30% of the total primary production in the Arctic (Hop et al., 2006). This leaves 70% of primary production available to microbial grazers.

Both dinoflagellates and ciliates can feed on large and chain-forming diatoms (Hansen and Calado, 1999; Olson and Strom, 2002; Aberle et al., 2007; Sherr et al., 2013). The results of dilution experiments in this study demonstrate that microbial grazers can remove a substantial portion of daily phytoplankton production even during the spring bloom. These data correspond to the previous studies in the Arctic seas (reviewed in Franzè and Lavrentyev, 2017, Table 3). The stimulating effect of ice cover on microzooplankton herbivory in this study is surprising, because in the adjacent Barents Sea, microzooplankton herbivory increased with temperature and was higher in the open waters than under the ice (Verity et al., 2002; Franzè and Lavrentyev, 2017). It is plausible that microzooplankton responded to the ice-induced changes in phytoplankton composition and/or dynamics. Overall, this study demonstrates the capacity of microzooplankton to control primary production in both ice-covered and open waters. For example, the experiments conducted at P1/P5 in May (−0.5 to 0°C, 90% ice cover) and August (6 to 6.3°C, open water) yielded similar depth-averaged grazing rates (0.14 and 0.12 d^{-1}, respectively). In both cases, ca. 50% of daily primary production was removed.

In two surface experiments (P4 and P7), microzooplankton consumed > 100% of primary production. This is not unusual (Calbet and Landry, 2004; Menden-Deuer et al., 2018) and likely reflects the dynamic equilibrium between phytoplankton growth and grazing (Irigoien et al., 2005) and, possibly, the effect of large predator removal. Herbivory, as measured in dilution experiments, is a community process. Based on microscopy, nauplii and other invertebrates were rare in our samples. The most likely contributors to the measured grazing rates were heterotrophic and mixotrophic pico- and nanoflagellates, which were abundant at the process stations, especially in the summer (up to 1500 cells mL^{-1}, Paulsen et al., 2016). Interestingly, in the latter study the flagellates grew faster (up to 0.53 d^{-1}) in <5 μm fraction, whereas their *Synechococcus* prey grew faster in <90 μm fraction, suggesting a picoplankton-nanoflagellate-microzooplankton-copepod trophic cascade.

Although the dilution experiments at P3-15 m technically failed because chlorophyll concentrations declined precipitously in the diluted treatment, it should be noted that colonial *P. pouchetii* formed > 90% of microscopic phytoplankton abundance at this site (Sanz-Martín et al., 2018). Microzooplankton can feed on *P. pouchetii* as evidenced by the outcome of dilution experiments at P3-40 m and P4 and published research (Verity et al., 2007; Grattepanche et al., 2011). However, the presence of colonial *P. pouchetii* is often reported in conjunction with low or insignificant herbivory rates in dilution experiments (Calbet et al., 2011; Stoecker et al., 2015; Menden-Deuer et al., 2018). In addition to forming large colonies, *P. pouchetii* can produce toxic polyunsaturated aldehydes (PUAs) such as 2-*trans*-4-*trans*-decadienal (Hansen et al., 2004). PUA impaired growth of some marine ciliates and dinoflagellates (Lavrentyev et al., 2015). Microzooplankton grew in both experiments at P3, albeit much faster in the seawater collected from 40 m (P/B: 0.29 vs. 0.11 d^{-1} at 15 m). Several abundant species were responsible for this difference (*G. spirale:* 1.08 vs. 0.39 d^{-1}; *P. bipes:* 0.88 vs. −0.69 d^{-1}; *M. rubrum:* 1.39 vs. 0.39 d^{-1}), whereas others were not (e.g., *Strombidium* sp.: 0.79 vs. 1.04 d^{-1}). However, the lack of PUA measurements does not allow us to untangle the possible effects of *Phaeocystis*-produced cytotoxins and temperature at different depths. This phenomenon should be investigated further, since *P. pouchetii* is a

very common and often dominant component of phytoplankton assemblages in the Arctic. In addition, dissolved PUA production by marine phytoplankton can create opportunities for bloom development by inhibiting herbivory and stimulating copepod predation on microzooplankton (Franzè et al., 2018).

Microzooplankton Growth and Production

Similar to microzooplankton in the Barents Sea (Franzè and Lavrentyev, 2014), on average one third of the microzooplankton community grew in any given experiments. The rest of the populations either declined or did not change significantly over 24 h. This asynchronisity in the growth of dominant species appears to reflect a general pattern of microzooplankton community dynamics, where multiple populations oscillate out of phase, whereas short-term incubations provide only a snapshot of these dynamics. The rapid species-specific growth rates of ciliates and dinoflagellates in our experiments support the idea that low temperatures do not constrain their growth more than that of their phytoplankton prey (Sherr et al., 2013; Menden-Deuer et al., 2018). Further, the ability of these protists to achieve their intrinsic maxima rapidly is likely an adaptation to the fluctuating and spatially heterogeneous environment (Franzè and Lavrentyev, 2014). Nevertheless, the growth response of microzooplankton community to temperature was evident, particularly at temperatures ≤ 0°C. Given the current climate change in the Arctic, it is likely that microzooplankton growth will increase in a warmer ocean leading to greater retention of carbon in the mixed layer (Franzè and Lavrentyev, 2017). At the same time, the growth-temperature equations resulting from our field experiments should be used with caution as they may reflect the indirect effects of other factors such as resource limitation (Rose and Caron, 2007) and/or intraguild predation (e.g., Franzè and Modigh, 2013).

Because microzooplankton growth rates were similar between May and August, we can apply the average rate of 0.23 d^{-1} calculated for AW to the depth-integrated (0–100 m) microzooplankton biomass in transect D. The resulting average production rate of 227 mg C m^{-2} d^{-1} combined with the growth gross efficiency of 30% commonly reported for zooplankton (Straile, 1997) yields a daily carbon demand of 756 mg C m^{-2} d^{-1}. Over the 4-month period from May to August microzooplankton production and carbon demand (27.9 and 93 g C m^{-2}, respectively) would equal 23 and 75% of the annual gross primary production in the eastern Fram Strait (123 g C m^{-2} y^{-1}, Forest et al., 2010). These calculations depend on primary production estimates, which vary from 80 to 180 g C m^{-2} y^{-1} in the WSC (Hop et al., 2006), and do not account for the effects of phytoplankton respiration and exudation, mixotrophy, bacterivory, and copepod predation on microzooplankton. However, they correspond to the average microzooplankton herbivory impact in this study and illustrate the scale of carbon flux through the microbial food web in the Fram Strait and the Arctic Ocean shelf. For comparison, *C. finmarchicus* secondary production in the Atlantic inflow was estimated at 2–4 g C m^{-2} y^{-1} (Slagstad et al., 2011) or 7 to 14% of microzooplankton production estimated in this study. Svensen et al. (2019) estimated *C. finmarchicus* production at 11 to 23% of microzooplankton production at the process stations. Further, microzooplankton growth in the Arctic is not limited to May through August. Protists remain active during the polar winter (Druzhkov and Druzhkova, 1998; Møller et al., 2006) and form considerable biomass in the early spring before the diatom bloom (Levinsen et al., 2000b; Seuthe et al., 2011). Therefore, their potential role in polar pelagic food webs may be even greater than suggested by the above estimates.

CONCLUSION

Ciliates and dinoflagellates are an important component of the pelagic food web in both the Atlantic waters of WSC and the ice-covered Arctic shelf waters; their biomass is comparable with that of dominant copepods. Due to their rapid biomass turnover, microzooplankton can produce an order of magnitude more carbon than net zooplankton. Mixotrophic ciliates can form surface blooms and contribute substantially to chlorophyll *a* in the mixed layer, but their role remains to be fully understood. Although microzooplankton biomass and composition displayed strong seasonality, their herbivory remained a major factor controlling primary production except during the peak of colonial *P. pouchetii*. Based on their critical role in the pelagic carbon cycle in the Fram Strait and other polar seas systems, microzooplankton must become a regular component of monitoring programs and models focused on the climate change effects in the Arctic.

AUTHOR CONTRIBUTIONS

PL designed and conducted the experiments, analyzed data, and wrote the manuscript. GF designed and conducted the experiments, analyzed data, and prepared the figures. FM designed experimental equipment and conducted the experiments.

FUNDING

This study was funded by the National Science Foundation (Award OCE-1357168) and the University of Akron.

ACKNOWLEDGMENTS

We are grateful to the Carbon Bridge project and the University of Tromsø for letting us join their research cruises to the Fram Strait and the Arctic Ocean. We also thank Marit Reigstad, Lena Seuthe, Camilla Svensen, and the captain and crew of the R/Vs Helmer Hanssen for their logistical support and field assistance. The two reviewers provided helpful criticisms and suggestions.

REFERENCES

Aberle, N., Lengfellner, K., and Sommer, U. (2007). Spring bloom succession, grazing impact and herbivore selectivity of ciliate communities in response to winter warming. *Oecologia* 150, 668–681. doi: 10.1007/s00442-006-0540-y

Arar, E. J., and Collins, G. B. (1997). *Method 445.0 In Vitro Determination of Chlorophyll a and Pheophytin ain Marine and Freshwater Algae by Fluorescence*. Cincinnati, OH: National Exposure Research Laboratory.

Basedow, S. L., Sundfjord, A., von Appen, W. J., Halvorsen, E., Kwasniewski, S., and Reigstad, M. (2018). Seasonal variation in transport of zooplankton into the arctic basin through the atlantic gateway, fram strait. *Front. Mar. Sci.* 5:194, doi: 10.3389/fmars.2018.00194

Brown, Z. W., and Arrigo, K. R. (2012). Contrasting trends in sea ice and primary production in the Bering Sea and Arctic Ocean. *ICES J. Mar. Sci.* 69, 1180–1193. doi: 10.1093/icesjms/fss113

Calbet, A., and Landry, M. R. (2004). Phytoplankton growth, microzooplankton grazing, and carbon cycling in marine systems. *Limnol. Oceanogr.* 49, 51–57. doi: 10.3354/meps09343

Calbet, A., Saiz, E., Almeda, R., Movilla, J. I., and Alcaraz, M. (2011). Low microzooplankton grazing rates in the Arctic Ocean during a *Phaeocystis pouchetii* bloom (Summer 2007): fact or artifact of the dilution technique? *J. Plankton Res.* 33, 687–701. doi: 10.1093/plankt/fbq142

Campbell, R. G., Sherr, E. B., Ashjian, C. J., Plourde, S., Sherr, B. F., Hill, V., et al. (2009). Mesozooplankton prey preference and grazing impact in the western Arctic Ocean. *Deep Sea Res. Part II Top. Stud. Oceanogr.* 56, 1274–1289. doi: 10.1016/j.dsr2.2008.10.027

Caron, D. A., and Hutchins, D. A. (2013). The effects of changing climate on microzooplankton grazing and community structure: drivers, predictions and knowledge gaps. *J. Plankton Res.* 35, 235–252. doi: 10.1093/plankt/fbs091

Chen, B. Z. (2015). Assessing the accuracy of the "two-point" dilution technique. *Limnol. Oceanogr. Methods* 13, 521–526. doi: 10.1002/lom3.10044

Cokelet, E. D., Tervalon, N., and Bellingham, J. G. (2008). Hydrography of the west spitsbergen current, svalbard branch: autumn 2001. *J. Geophys. Res. Oceans* 113, 1-16. doi: 10.1029/2007JC004150

Corell, R. W. (2006). Challenges of climate change: an arctic perspective. *Ambio* 35, 148–152. doi: 10.1579/0044-7447200635

Dolan, J. R., and Perez, M. T. (2000). Costs, benefits and characteristics of mixotrophy in marine oligotrichs. *Freshw. Biol.* 45, 227–238. doi: 10.1046/j.1365-2427.2000.00659.x

Druzhkov, N. V., and Druzhkova, E. I. (1998). "Microzooplankton of the Pechora and Barents seas in the end of winter (in Russian)," in *Biology and Oceanography of the Kara and Barents Seas (along the Northern Sea Route)*, ed. G. G. Matishov (Moscow: Russian Academy of Sciences), 120–138.

Forest, A., Wassmann, P., Slagstad, D., Bauerfeind, E., Nöthig, E. M., and Klages, M. (2010). Relationships between primary production and vertical particle export at the Atlantic-Arctic boundary (Fram Strait, HAUSGARTEN). *Polar Biol.* 33, 1733–1746. doi: 10.1007/s00300-010-0855-853

Franzè, G., and Lavrentyev, P. J. (2014). Microzooplankton growth rates examined across a temperature gradient in the Barents Sea. *PLoS One* 9:e86429. doi: 10.1371/journal.pone.0086429

Franzè, G., and Lavrentyev, P. J. (2017). Microbial food web structure and dynamics across a natural temperature gradient in a productive polar shelf system. *Mar. Ecol. Prog. Series* 569, 89–102. doi: 10.3354/meps12072

Franzè, G., and Modigh, M. (2013). Experimental evidence for internal predation in microzooplankton communities. *Mar. Biol.* 160, 3103–3112. doi: 10.1007/s00227-013-2298-2291

Franzè, G., Pierson, J. J., Stoecker, D. K., and Lavrentyev, P. J. (2018). Diatom-produced allelochemicals trigger trophic cascades in the planktonic food web. *Limnol. Oceanogr.* 63, 1093–1108. doi: 10.1002/lno.10756

Grattepanche, J. D., Vincent, D., Breton, E., and Christaki, U. (2011). Microzooplankton herbivory during the diatom-phaeocystis spring succession in the eastern english channel. *J. Exp. Mar. Biol. Ecol.* 404, 87–97. doi: 10.1016/j.jembe.2011.04.004

Hansen, B., Christiansen, S., and Pedersen, G. (1996). Plankton dynamics in the marginal ice zone of the central Barents Sea during spring: carbon flow and structure of the grazer food chain. *Polar Biol.* 16, 115–128. doi: 10.1007/BF02390432

Hansen, E., Ernstsen, A., and Eilertsen, H. C. (2004). Isolation and characterisation of a cytotoxic polyunsaturated aldehyde from the marine phytoplankter *Phaeocystis pouchetii* (Hariot) Lagerheim. *Toxicology* 199, 207–217. doi: 10.1016/j.tox.2004.02.026

Hansen, P. J., and Calado, A. J. (1999). Phagotrophic mechanisms and prey selection in free-living dinoflagellates. *J. Eukaryot. Microbiol.* 46, 382–389. doi: 10.1111/j.1550-7408.1999.tb04617.x

Hop, H., Falk-Petersen, S., Svendsen, H., Kwasniewski, S., Pavlov, V., Pavlova, O., et al. (2006). Physical and biological characteristics of the pelagic system across Fram Strait to Kongsfjorden. *Prog Oceanogr.* 71, 182–231. doi: 10.1016/j.pocean.2006.09.007

IPCC (2013). "Climate Change 2013" in *The Physical Science Basis. Contribution of Working Group I to the Fifth Assessment Report of the Intergovernmental Panel on Climate Change* [T.F. Stocker, D. Qin, G.-K. Plattner, M. Tignor, S.K. Allen, J. Boschung, A. Nauels, Y. Xia, V. Bex and P.M. Midgley (eds.)]. Cambridge: Cambridge University Press, 1535.

Irigoien, X., Flynn, K. J., and Harris, R. P. (2005). Phytoplankton blooms: a 'loophole' in microzooplankton grazing impact? *J. Plankton Res.* 27, 313–321. doi: 10.1093/plankt/fbi011

Kosobokova, K., and Hirche, H. J. (2009). Biomass of zooplankton in the eastern Arctic Ocean - a base line study. *Prog. Oceanogr.* 82, 265–280. doi: 10.1016/j.pocean.2009.07.006

Kwok, R., and Rothrock, D. A. (2009). Decline in Arctic sea ice thickness from submarine and ICESat records: 1958-2008. *Geophys. Res. Lett.* 36, 1–5. doi: 10.1029/2009gl039035

Landry, M., Brown, S. L., Rii, Y., Selph, K., Bidigare, R., Yang, E., et al. (2008). Depth-stratified phytoplankton dynamics in Cyclone Opal, a subtropical mesoscale eddy. *Deep Sea Res. Part II Top. Stud. Oceanogr.* 55, 1348–1359. doi: 10.1016/j.dsr2.2008.02.001

Lavrentyev, P. J. (2012). Microzooplankton studies in the Kara Sea during the Yamal-Arctic 2012 expedition. *Russian Polar Res.* 10, 24–26.

Lavrentyev, P. J., Franzè, G., Pierson, J. J., and Stoecker, D. K. (2015). The effect of dissolved polyunsaturated aldehydes on microzooplankton growth rates in the Chesapeake Bay and Atlantic coastal waters. *Mar. Biol.* 13, 2834–2856. doi: 10.3390/md13052834

Levinsen, H., Nielsen, T. G., and Hansen, B. W. (2000a). Annual succession of marine pelagic protozoans in Disko Bay. West Greenland, with emphasis on winter dynamics. *Mar. Ecol. Prog. Series* 206, 119–134. doi: 10.3354/meps206119

Levinsen, H., Turner, J. T., Nielsen, T. G., and Hansen, B. W. (2000b). On the trophic coupling between protists and copepods in arctic marine ecosystems. *Mar. Ecol. Prog. Series* 204, 65–77. doi: 10.3354/meps204065

Li, W. K. W., McLaughlin, F. A., Lovejoy, C., and Carmack, E. C. (2009). Smallest algae thrive as the Arctic Ocean freshens. *Science* 326, 539–539. doi: 10.1126/science.1179798

Lind, S., and Ingvaldsen, R. B. (2012). Variability and impacts of Atlantic Water entering the Barents Sea from the north. *Deep Sea Res. Part I Oceanogr. Res. Papers* 62, 70–88. doi: 10.1016/j.dsr.2011.12.007

Litchman, E., Ohman, M. D., and Kiorboe, T. (2013). Trait-based approaches to zooplankton communities. *J. Plankton Res.* 35, 473–484. doi: 10.1093/plankt/fbt019

Lovejoy, C., Legendre, L., Martineau, M. J., Bacle, J., and von Quillfeldt, C. H. (2002). Distribution of phytoplankton and other protists in the North Water. *Deep Sea Res. Part II Top. Stud. Oceanogr.* 49, 5027–5047. doi: 10.1016/S0967-0645(02)00176-175

McBride, M. M., Dalpadado, P., Drinkwater, K. F., Godo, O. R., Hobday, A. J., Hollowed, A. B., et al. (2014). Krill, climate, and contrasting future scenarios for Arctic and Antarctic fisheries. *ICES J. Mar. Sci.* 71, 1934–1955. doi: 10.1093/icesjms/fsu002

McManus, G. B., Schoener, D. M., and Haberlandt, K. (2012). Chloroplast symbiosis in a marine ciliate: ecophysiology and the risks and rewards of hosting foreign organelles. *Front. Microbiol.* 3:321. doi: 10.3389/fmicb.2012.00321

Menden-Deuer, S., Lawrence, C. A., and Franzè, G. (2018). Herbivorous protist growth and grazing rates at in situ and artificially elevated temperatures during an Arctic phytoplankton spring bloom. *Peer J.* 6:e5264. doi: 10.7717/peerj.5264

Menden-Deuer, S., and Lessard, E. J. (2000). Carbon to volume relationships for dinoflagellates, diatoms, and other protist plankton. *Limnol. Oceanogr.* 45, 569–579. doi: 10.4319/lo.2000.45.3.0569

Møller, E. F., Nielsen, T. G., and Richardson, K. (2006). The zooplankton community in the Greenland Sea: composition and role in carbon turnover. *Deep Sea Res. Part I Oceanogr. Res. Papers* 53, 76–93. doi: 10.1016/j.dsr.2005.09.007

Montagnes, D. J. S., Berges, J. A., Harrison, P. J., and Taylor, F. J. R. (1994). Estimating carbon, nitrogen, protein, and chlorophyll-a from volume in marine phytoplankton. *Limnol. Oceanogr.* 39, 1044–1060. doi: 10.4319/lo.1994.39.5.1044

Morison, F., and Menden-Deuer, S. (2017). Doing more with less? Balancing sampling resolution and effort in measurements of protistan growth and grazing-rates. *Limnol. Oceanogr. Methods* 15, 794–809. doi: 10.1002/lom3.10200

Nöthig, E., Bracher, A., Engel, A., Metfies, K., Niehoff, B., Peeken, I., et al. (2015). Summertime plankton ecology in Fram Strait—a compilation of long- and short-term observations. *Polar Res.* 34:23349, doi: 10.3402/polar.v34.23349

Ohman, M. D., and Runge, J. A. (1994). Sustained fecundity when phytoplankton resources are in short supply: omnivory by *Calanus finmarchicus* in the Gulf of St. Lawrence. *Limnol. Oceanogr.* 39, 21–36. doi: 10.4319/lo.1994.39.1.0021

Olson, M. B., and Strom, S. L. (2002). Phytoplankton growth, microzooplankton herbivory and community structure in the southeast Bering Sea: insight into the formation and temporal persistence of an *Emiliania huxleyi* bloom. *Deep Sea Res. Part II Top. Stud. Oceanogr.* 49, 5969–5990. doi: 10.1016/S0967-0645(02)00329-326

Paulsen, M. L., Doré, H., Garczarek, L., Seuthe, L., Müller, O., Sandaa, R. A., et al. (2016). *Synechococcus* in the Atlantic Gateway to the Arctic Ocean. *Front. Mar. Sci.* 3:191, doi: 10.3389/fmars.2016.00191

Peltomaa, E., and Johnson, M. D. (2017). *Mesodinium rubrum* exhibits genus-level but not species-level cryptophyte prey selection. *Aquat. Microb. Ecol.* 78, 147–159. doi: 10.3354/ame01809

Pnyushkov, A. V., Polyakov, I. V., Ivanov, V. V., Aksenov, Y., Coward, A. C., Janout, M., et al. (2015). Structure and variability of the boundary current in the Eurasian Basin of the Arctic Ocean. *Deep Sea Res. Part I Oceanogr. Res. Papers* 101, 80–97. doi: 10.1016/j.dsr.2015.03.001

Polyakov, I. V., Pnyushkov, A. V., and Timokhov, L. A. (2012). Warming of the Intermediate Atlantic Water of the Arctic Ocean in the 2000s. *J. Clim.*. 25, 8362–8370. doi: 10.1175/JCLI-D-12-00266.1

Putt, M. (1990). Abundance, chlorophyll content and photosynthetic rates of ciliates in the Nordic Seas during summer. *Deep Sea Res. Part I Oceanogr. Res. Papers* 37, 1713–1731. doi: 10.1016/0198-0149(90)90073-90075

Putt, M., and Stoecker, D. K. (1989). An experimentally determined carbon:volume ratio for marine oligotrichous ciliates from estuarine and coastal waters. *Limnol. Oceanogr.* 34, 1097–1103. doi: 10.4319/lo.1989.34.6.1097

Randelhoff, A., Reigstad, M., Chierici, M., Sundfjord, A., Ivanov, V., Cape, M., et al. (2018). Seasonality of the physical and biogeochemical hydrography in the inflow to the Arctic Ocean through Fram Strait. *Front. Mar. Sci.* 5:224, doi: 10.3389/fmars.2018.00224

Rat'kova, T. N., and Wassmann, P. (2002). Seasonal variation and spatial distribution of phyto- and protozooplankton in the central Barents Sea. *J. Mar. Syst.* 38, 47–75. doi: 10.1016/S0924-7963(02)00169-160

Ray, J. L., Skaar, K. S., Simonelli, P., Larsen, A., Sazhin, A., Jakobsen, H. H., et al. (2016). Molecular gut content analysis demonstrates that *Calanus* grazing on *Phaeocystis pouchetii* and *Skeletonema marinoi* is sensitive to bloom phase but not prey density. *Mar. Ecol. Prog. Series* 542, 63–77. doi: 10.3354/meps11560

Rose, J. M., and Caron, D. A. (2007). Does low temperature constrain the growth rates of heterotrophic protists? Evidence and implications for algal blooms in cold waters. *Limnol. Oceanogr.* 52, 886–895. doi: 10.4319/lo.2007.52.2.0886

Saiz, E., and Calbet, A. (2011). Copepod feeding in the ocean: scaling patterns, composition of their diet and the bias of estimates due to microzooplankton grazing during incubations. *Hydrobiologia* 666, 181–196. doi: 10.1007/s10750-010-0421-426

Saiz, E., Calbet, A., Isari, S., Anto, M., Velasco, E. M., Almeda, R., et al. (2013). Zooplankton distribution and feeding in the Arctic Ocean during a *Phaeocystis pouchetii* bloom. *Deep Sea Res. Part I Oceanogr. Res. Papers* 72, 17–33. doi: 10.1016/j.dsr.2012.10.003

Sanz-Martín, M., Chierici, M., Mesa, E., Carrillo-de-Albornoz, P., Delgado-Huertas, A., Agustí, S., et al. (2018). Episodic arctic CO2 limitation in the West Svalbard shelf. *Front. Mar. Sci.* 5:221, doi: 10.3389/fmars.2018.00221

Sarmento, H., Montoya, J. M., Vazquez-Dominguez, E., Vaqué, D., and Gasol, J. M. (2010). Warming effects on marine microbial food web processes: how far can we go when it comes to predictions? *Philos. Trans. R Soc. B Biol. Sci.* 365, 2137–2149. doi: 10.1098/rstb.2010.0045

Schauer, U., Fahrbach, E., Osterhus, S., and Rohardt, G. (2004). Arctic warming through the Fram Strait: oceanic heat transport from 3 years of measurements. *J. Geophys. Res. Oceans* 109, doi: 10.1029/2003JC001823

Schmoker, C., Hernandez-Leon, S., and Calbet, A. (2013). Microzooplankton grazing in the oceans: impacts, data variability, knowledge gaps and future directions. *J. Plankton Res.* 35, 691–706. doi: 10.1093/plankt/fbt023

Schoener, D. M., and McManus, G. B. (2012). Plastid retention, use, and replacement in a kleptoplastidic ciliate. *Aquat. Microb. Ecol.* 7, 177–187. doi: 10.3354/ame01601

Seuthe, L., Topper, B., Reigstad, M., Thyrhaug, R., and Vaquer-Sunyer, R. (2011). Microbial communities and processes in ice-covered Arctic waters of the northwestern Fram Strait (75 to 80 degrees N) during the vernal pre-bloom phase. *Aquat. Microb. Ecol.* 64, 253–266. doi: 10.3354/Ame01525

Sherr, E. B., Sherr, B. F., and Hartz, A. J. (2009). Microzooplankton grazing impact in the Western Arctic Ocean. *Deep Sea Res. Part II Top. Stud. Oceanogr.* 56, 1264–1273. doi: 10.1016/j.dsr2.2008.10.036

Sherr, E. B., Sherr, B. F., and Ross, C. (2013). Microzooplankton grazing impact in the Bering Sea during spring sea ice conditions. *Deep Sea Res. Part II Top. Stud. Oceanogr.* doi: 10.1016/j.dsr2.2013.03.019

Slagstad, D., Ellingsen, I. H., and Wassmann, P. (2011). Evaluating primary and secondary production in an Arctic Ocean void of summer sea ice: an experimental simulation approach. *Prog. Oceanogr.* 90, 117–131. doi: 10.1016/j.pocean.2011.02.009

Smetacek, V. (1999). Diatoms and the ocean carbon cycle. *Protist* 150, 25–32. doi: 10.1016/S1434-4610(99)70006-70004

Stoecker, D. K., and Lavrentyev, P. J. (2018). Mixotrophic plankton in the Polar Seas: a pan-Arctic review. *Front. Mar. Sci.* 5:292, doi: 10.3389/fmars.2018.00292

Stoecker, D. K., Nejstgaard, J. C., Madhusoodhanan, R., Pohnert, G., Wolfram, S., Jakobsen, H. H., et al. (2015). Underestimation of microzooplankton grazing in dilution experiments due to inhibition of phytoplankton growth. *Limnol. Oceanogr.* 60, 1426–1438. doi: 10.1002/lno.10106

Stoecker, D. K., Silver, M. W., Michaels, A. E., and Davis, L. H. (1988). Enslavement of algal chloroplasts by four *Strombidium* spp. (ciliophora. oligotrichida). *Mar. Microb. Food Webs* 3, 79–100.

Stoecker, D. K., Weigel, A., and Goes, J. I. (2014a). Microzooplankton grazing in the Eastern Bering Sea in summer. *Deep Sea Res. Part II Top. Stud. Oceanogr.* 109, 145–156. doi: 10.1016/j.dsr2.2013.09.017

Stoecker, D. K., Weigel, A. C., Stockwell, D. A., and Lomas, M. W. (2014b). Microzooplankton: abundance, biomass and contribution to chlorophyll in the Eastern Bering Sea in summer. *Deep Sea Res. Part II Top. Stud. Oceanogr.* 109, 134–144. doi: 10.1016/j.dsr2.2013.09.007

Straile, D. (1997). Gross growth efficiencies of protozoan and metazoan zooplankton and their dependence on food concentration, predator-prey weight ratio, and taxonomic group. *Limnol. Oceanogr.* 42, 1375–1385. doi: 10.4319/lo.1997.42.6.1375

Strom, S. L., and Fredrickson, K. A. (2008). Intense stratification leads to phytoplankton nutrient limitation and reduced microzooplankton grazing in the southeastern Bering Sea. *Deep Sea Res. Part II Top. Stud. Oceanogr.* 55, 1761–1774. doi: 10.1016/j.dsr2.2008.04.008

Svensen, C., Halvorsen, E., Vernet, M., Franzè, G., Dmoch, K., Lavrentyev, P. J., et al. (2019). Zooplankton communities associated with new and regenerated production in the Atlantic inflow north of Svalbard. *Front. Mar. Sci.*

Verity, P. G., Wassmann, P., Frischer, M. E., Howard-Jones, M. H., and Allen, A. E. (2002). Grazing of phytoplankton by microzooplankton in the Barents Sea during early summer. *J. Mar. Syst.* 38, 109–123. doi: 10.1016/S0924-7963(02)00172-0

Verity, P. G., Zirbel, M. J., and Nejstgaard, J. C. (2007). Formation of very young colonies by *Phaeocystis pouchetii* from western Norway. *Aquat. Microb. Ecol.* 47, 267–274. doi: 10.3354/ame047267

Ward, B. A., and Follows, M. J. (2016). Marine mixotrophy increases trophic transfer efficiency, mean organism size and vertical carbon flux. *Proc. Nat. Acad. Sci.* 113, 2958–2963. doi: 10.1073/pnas.1517118113

Wassmann, P., and Lenton, T. M. (2012). Arctic tipping points in an Earth system perspective. *Ambio* 41, 1–9. doi: 10.1007/s13280-011-0230-239

Wassmann, P., and Reigstad, M. (2011). Future Arctic Ocean seasonal ice zones and implications for pelagic-benthic coupling. *Oceanography* 24, 220–231. doi: 10.5670/oceanog.2011.74

Conflict of Interest Statement: The authors declare that the research was conducted in the absence of any commercial or financial relationships that could be construed as a potential conflict of interest.